

## AM1 Electron Density and NMR Spectral Studies of Carotenoids with a Strong Terminal Electron Acceptor

Elli S. Hand, Kenneth A. Belmore and Lowell D. Kispert\*

Chemistry Department, Box 870336, University of Alabama, Tuscaloosa, AL 35487, USA

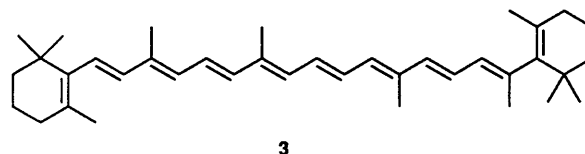
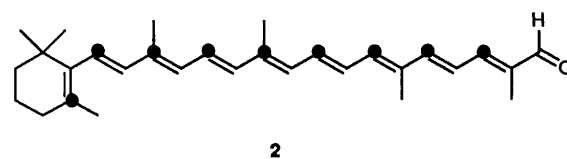
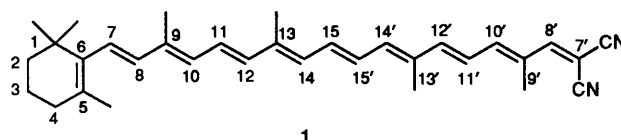
NMR spectral analyses of 7',7'-dicyano-7'-apo- $\beta$ -carotene (**1**), which was synthesized to assess the effect of a terminal strong electron acceptor on the structure of carotenoids and the molecular features which control their photochemical properties, are presented. AM1 Molecular orbital calculated electron density differences for **1** and 8'-apo- $\beta$ -caroten-8'-al (**2**) have been found to correlate with the differences in  $^{13}\text{C}$  NMR chemical shifts using  $\beta$ -carotene (**3**) as a reference.

Carotenoids are important in a number of biological contexts.<sup>1,2</sup> For example, they act as protective agents against photosensitization by the photosynthetic organism's own chlorophyll. This is achieved by transferring the excited singlet state energy of oxygen or the chlorophyll triplet state energy to the carotenoid-excited triplet state. Carotenoids serve an antenna function in the wavelength region 350–550 nm (where chlorophyll does not absorb),<sup>1</sup> and are important in other areas as well.<sup>2</sup>  $\beta$ -Carotene (**3**) quenches singlet oxygen, and can inhibit the formation of free radicals.<sup>3</sup> Exposure of photosystem II to short light flashes causes the formation of carotenoid cation free radicals.<sup>4</sup> The IR signal due to these cation radicals increases dramatically when the chloroplasts are treated with chemicals that inhibit oxygen evolution.<sup>4</sup> Carotenoids act as electron donors, and may possibly play a role in electron transport in some systems.

About 600 naturally-occurring carotenoids are known, but the relationship between (i) the different structures and substituents attached to the polyene chain and (ii) the function of the compound is, in most cases, not understood. These relationships cannot be elucidated without a broad information base, and, in this context, it is vital to learn more about the physical properties of carotenoids.

For instance, studies have shown<sup>5</sup> that carotenoids which possess polar functional groups can be attached to a photosynthetic reaction centre in a way which increases efficient triplet energy transfer over that of carotenoids without polar groups. Although these studies have been very useful, further study is needed to refine the relation between the substituent polarity, the proper geometry or position and the triplet energy transfer mechanism. Thus, we have synthesized an asymmetric and highly polarizable carotenoid, all-*trans*-7',7'-dicyano-7'-apo- $\beta$ -carotene (**1**) and determined its structure by 1D and 2D NMR measurements. We have also calculated AM1 ground state electron densities ( $q$ ) to interpret the NMR chemical shift differences of the chain carbon atoms of **1** and 8'-apo- $\beta$ -caroten-8'-al (**2**) relative to  $q$  and  $\delta$  of the symmetric nonpolar  $\beta$ -carotene. Previously AM1 calculations were used in this laboratory to interpret the excited state properties of **1** as a function of solvent relative permittivity and temperature (7.4–295 K).<sup>6</sup> Electron-withdrawing or -releasing groups in conjugation with the  $\pi$ -system of the polyene chain induce dipole moments in carotenoids and have considerable influence on their properties. For example, the dipole moment of compound **1** changes between the electronic ground and excited states.<sup>6</sup> On excitation, a carotenoid can undergo structural changes, especially in the backbone carbon-carbon bond lengths.<sup>6,7</sup> Such changes were predicted to occur in compound **1** by geometry-optimized AM1 calculations.<sup>6</sup> Although these calculations support the picosecond measurements, and show

that both  $S_1$  and  $S_2$  are highly polar excited states, further calibration of the AM1 approximation for carotenoids by independent physical measurements is warranted. The analysis of the NMR spectra and the synthesis of **1** and the interpretation of the AM1 electron densities are described.



### Results and Discussion

**Synthesis and Some Properties of 1.**—The dicyano compound was prepared by piperidine-catalysed condensation of **2** with excess malononitrile in benzene.<sup>†</sup> Purified samples, stored in a desiccator (or in vacuum-sealed ampoules) at 4 °C (or less) in the dark, were stable for at least 6 months. At ambient temperatures, the solid, kept under nitrogen but exposed to light, or in deuteriochloroform solution protected against light, gradually decomposed. Prolonged exposure to silica gel, particularly in the presence of air, light and/or heat, led to extensive decomposition. The elemental composition was established by high resolution mass spectrometry (HRMS); a scan from  $m/z$  50–500 showed the molecular ion to be the base peak, implying considerable stability of the radical cation. In chloroform compound **1** has a broad absorption band centred at 562 nm, as compared to previously reported<sup>6</sup> maxima at 530

<sup>†</sup> Compound **1** has been previously prepared in methanol with sodium methoxide catalysis,<sup>8</sup> not methanolic pyridine as inadvertently reported;<sup>6</sup> in our hands pyridine failed to catalyse this reaction. One other citation of **1** is in the patent literature.<sup>9</sup>

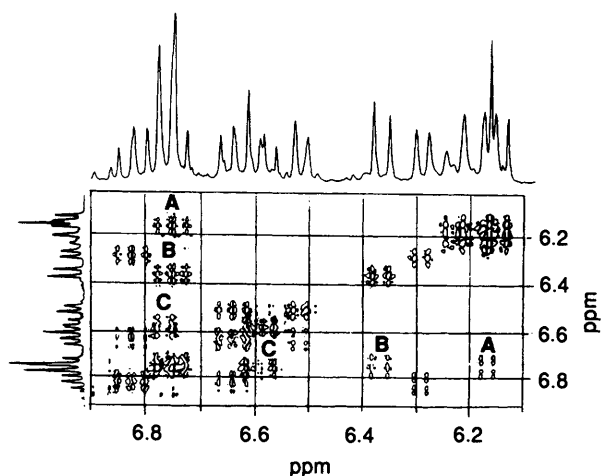


Fig. 1 Selected olefinic region of the 2D H, H-COSY 500 MHz spectrum of **1** (improperly phased by 90° in F1) in CDCl<sub>3</sub> at 27 °C. For cross-peak identification (A–C), see text.

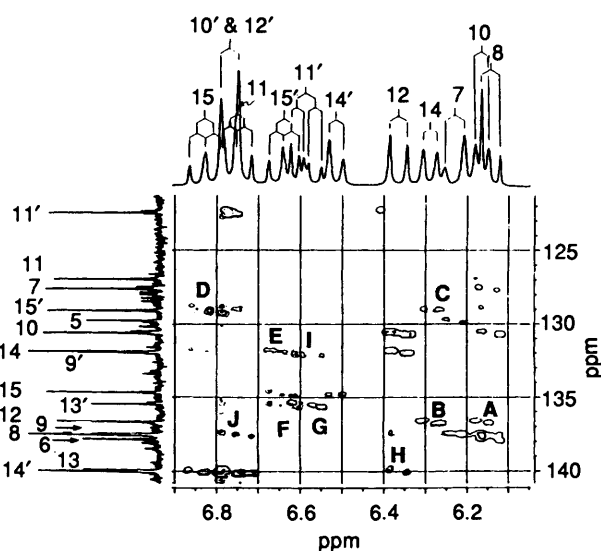


Fig. 2 Selected portion of a contour plot of the 2D H, C-HMBC spectrum of **1** in CDCl<sub>3</sub> at 27 °C and assignments of chemical shifts. Projections along the axes are 1D spectra obtained at 360 MHz for <sup>1</sup>H and 90 MHz for <sup>13</sup>C. For cross-peak identification (A–J), see text.

nm in acetonitrile and 545 nm in toluene. For reference, the aldehyde **2** shows an intense band at very much lower wavelength, 453 nm in CHCl<sub>3</sub>.

**NMR Spectral Analyses.**—Selected regions of the 1D proton and carbon spectra of **1** are shown in Figs. 1–3, bordering the 2D correlation spectra. The usual numbering for carotenoids is indicated in structure **1**, but methyl groups will be identified by the carbon to which they are attached. As is often the case with long-chain polyenes, <sup>1</sup>H NMR spectra showed extensive overlap of the signals due to the 13 olefinic protons, even at high field strength (Fig. 1, 500 MHz and Figs. 2 and 3, 360 MHz). The chemical shifts of only four of these could be deduced from the 1D spectrum: 8'-H gives rise to a singlet at low field and 7-H and 8-H display the AB pattern, overlapping with the AX pattern of 10-H (near 6.2 ppm) that is commonly observed in spectra of carotenoids containing a terminal electron-withdrawing and a terminal 'β'-substituent [6-(1,1,5-trimethylcyclohex-5-ene)].<sup>10</sup> Nuclear Overhauser enhancement (NOE) studies confirmed the assignments of 7-H and 8-H and established the chemical shifts and multiplicities of 10'-H and 11'-H (Table 1).

Chemical shifts and multiplicities of three other protons

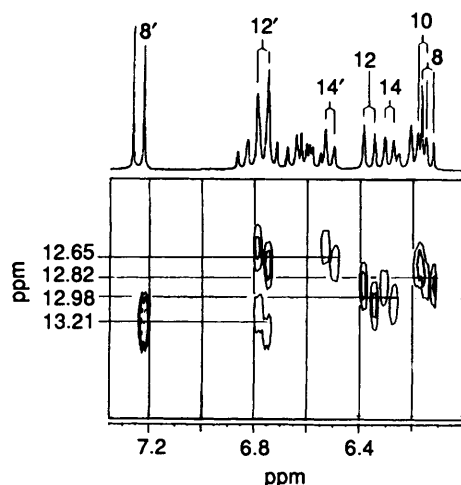


Fig. 3 Fold-in region of chain methyl carbon/olefinic proton cross-peaks of the HMBC spectrum of **1**. Numbers on the left axis are actual <sup>13</sup>C chemical shifts.

Table 1 Nuclear Overhauser effects in compound **1**

Irradiation	Proton(s)	δ	Enhancement <sup>a</sup>		
			Proton	δ	%
1-CH <sub>3</sub>	1.04	2-H	1.47 (m)	6.3	
		7-H	6.23 (d)	6.7	
		8-H	6.15 (d)	4.3	
5-CH <sub>3</sub>	1.74	4-H	2.02 (m)	2.6	
		7-H	6.23 (d)	2.1	
		8-H	6.15 (d)	3.2	
9, 13, 13'-CH <sub>3</sub> 's (and 4-H)	~1.99	7-H	6.23 (d)	7.0	
		11, 11', 15, 15'-H	6.55– 6.87 (m)	up to ca. 7	
		11'-H	6.58 (dd)	4.0	
9'-CH <sub>3</sub>	2.27	11'-H	6.58 (dd)	4.0	
8'-H	7.22	10'-H	6.76 (d)	3.4	

<sup>a</sup> From NOE difference spectra (360 MHz); other signals (not shown) were enhanced by <2%.

were obtained from a <sup>1</sup>H, <sup>1</sup>H COSY spectrum (Fig. 1). The cross-peak (A) of 10-H identifies 11-H (d,d), which is also coupled to 12-H (d, cross-peak B). Since 11'-H is coupled to 10'-H and 12'-H, but only one cross-peak (C) is observed, H-10' and H-12' must have (nearly) identical chemical shifts. Cross-peaks of protons not yet identified (14-, 15-, 15', 14'-H) establish which signals are due to neighbouring protons (14-H/15-H and 14'-H/15'-H), but do not permit specific identification. The assignments indicated for these protons (Fig. 2) were ultimately deduced from heteronuclear multiple bond correlation (HMBC) spectra (see below).

In the aliphatic region, only the chain methyl proton chemical shifts differed somewhat from those of β-carotene<sup>10</sup> and were derived from heteronuclear (<sup>1</sup>J<sub>CH</sub>) correlation (HETCOR) spectra after the <sup>13</sup>C chemical shifts were established by HMBC.

Proton chemical shifts and coupling constants for **1–3** are summarized in Table 2. Values for protons whose signals overlap were estimated from the COSY cross-peaks. Compared to **3**, protons attached to carbons which bear a positive charge in formal resonance structures (indicated by dots in structure **2**) are deshielded to a somewhat greater extent in **1** than in **2** (except for 10'-H). Similarity of the proton chemical shifts of **1** and **2** and the results of NOE studies indicate that **1** has the all-*trans* structure. The fact that corresponding coupling constants of **1–3** are about the same supports this conclusion.

It may be noted that  $J_{11,12}$  (~ $J_{11',12'}$ ) is considerably larger than  $J_{14,15}$  (~ $J_{14',15'}$ ); the magnitude is thus diagnostic for the doublets 12(12')-H and 14(14')-H. Further, it is expected that

**Table 2**  $^1\text{H}$  NMR Data ( $\text{CDCl}_3$ ) for compounds 1–3

Atom	$\delta$			Atom	$J_{\text{HH}}$ (Hz)		
	1 <sup>a</sup>	2 <sup>b</sup>	3 <sup>c</sup>		1	2	3 <sup>c</sup>
7	6.23	6.20	6.20	7, 8	16.2	16.2	16.1
8	6.15	6.14	6.14	10, 11	11.3	11.5	10.8
10	6.17	6.16	6.16	11, 12	14.9	14.9	15.1
11	6.75	6.71	6.66	14, 15	11.8	11.7	11.8
12	6.37	6.36	6.36	15, 15'	14.9 <sup>d</sup>		14.4
14	6.29	6.27	6.26	14', 15'	11.9	11.6	
15	6.82	6.77	6.63	11', 12'	15.1 <sup>d</sup>	~ 15.1	
15'	6.64	6.64	(6.63)	10', 11'	11.0 <sup>d</sup>	10.8	
14'	6.52	6.45	(6.26)				
12'	6.77	6.74	(6.36)				
11'	6.59	6.66	(6.66)				
10'	6.77	6.94	(6.16)				

<sup>a</sup> Other  $\delta$  values: 8'-H, 7.22; 9- $\text{CH}_3$ , 1.99; 13- $\text{CH}_3$ , 2.02; 13'- $\text{CH}_3$ , 2.00; 9'- $\text{CH}_3$ , 2.27. 0.03 mol  $\text{dm}^{-3}$ ; 27 °C. <sup>b</sup> Ca. 0.06 mol  $\text{dm}^{-3}$ ; 27 °C; values are within  $\pm 0.02$  ppm of those reported in ref. 10, except 11' (reported 6.62 ppm). <sup>c</sup> From ref. 19; 0.06 mol  $\text{dm}^{-3}$ , 30 °C. <sup>d</sup> Estimated from COSY cross-peaks (Fig. 1).

the olefinic proton chemical shifts of other all-*trans* 7'-apo- $\beta$ -carotenes containing a terminal electron-withdrawing substituent will follow the observed order  $\delta$  8-H < 8', 10 < 10', 12 < 12', 14 < 14', 15' < 15, and 11' < 11 and that the differences ( $\Delta\delta$ ) between the pairs will decrease from left to right in this series.

A  $^{13}\text{C}$  NMR spectrum of **1** displayed 31 of the 33 possible signals; the two *gem*- $\text{CH}_3$  carbons gave rise to only one signal and C-7' [=C(CN)<sub>2</sub>] could not be identified. Less than half of the  $^{13}\text{C}$  chemical shifts could be directly assigned from cross-peaks in a HETCOR spectrum and the established proton chemical shifts. Analysis of 2D HMBC spectra led to identification of the others. The pulse sequence parameters were adjusted to maximize signals due to  $^1\text{H}$ ,  $^{13}\text{C}$  couplings of ca. 9 Hz (primarily  $^3J_{\text{CH}}$ ).<sup>11</sup> The full  $^1\text{H}$  range was acquired, but to improve digital resolution, the spectral width of  $^{13}\text{C}$  was restricted to the range (101–163 ppm) in which the olefinic carbons resonate. A portion of the contour plot is shown in Fig. 2.

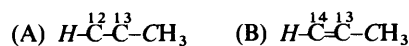
In this region, C-12, whose chemical shift was established by  $^1J_{\text{CH}}$  COSY, is expected to show cross-peaks due to long-range coupling with two protons, 10-H and 14-H; since  $\delta_{10\text{-H}}$  is known (cross-peak A), the other observed cross-peak (B) must be due to 14-H (d,  $\delta$  = 6.29). This assignment then permits identification of the signals due to 15-H, and 14'-H and 15'-H (linked by COSY, Fig. 1), as well as the corresponding  $^{13}\text{C}$  signals (linked by HETCOR, not shown). Other HMBC cross-peaks confirm the assignments; e.g., Fig. 2 shows coupling of 14-H/C-15' (C, three-bond), 15-H/C-15' (D, two-bond) and 15'-H/C-14 (E, three-bond).

The conclusion that  $\delta_{10\text{-H}} \sim \delta_{12\text{-H}}$ , reached from COSY (above), is verified by the HMBC data. For example, a cross-peak of C-8' ( $\delta$  = 161.75, not shown) with a  $^1\text{H}$  doublet ( $\delta$  = 6.77) can only be due to 10'-H. Further, the expected three-bond coupling of 10'-H and C-12' ( $\delta$  = 149.30, not shown) was observed, and C-12' also showed coupling to 14'-H (three-bond) and 11'-H (two-bond). The HETCOR cross-peak then linked 12'-H with C-12'.

While quaternary carbons are readily identified by the absence of their signals in DEPT and HETCOR spectra, assignment of these carbon chemical shifts rests almost exclusively on observed long-range couplings (HMBC) by which the connectivity sequence can be established. For compound **1**, all 10 of the quaternary carbons are  $\text{sp}^2$ , except the C-1 atom ( $\text{sp}^3$ ), which resonates at higher field ( $\delta$  = 34.28), and

their chemical shifts are deduced as follows. The carbon signals ( $\delta$  = 113.95 and 115.60, not shown), which display cross-peaks only with 8'-H (three-bond coupling), are due to the two non-equivalent CN carbons. The ring carbons, C-5 and C-6, are coupled not only with chain protons (7-H and 8-H, respectively), but also with ring protons, and their chemical shifts are similar to those reported for  $\beta$ -carotene.<sup>12</sup> The overlapping cross-peaks of 15'-H (F) and 11'-H (G) with the same carbon signal identify C-13' (three-bond couplings). 12-H shows a cross-peak (H) which must be due to coupling with C-13. [Other cross peaks in the  $^1\text{H}$  range 6.9–6.7 ppm with the two  $^{13}\text{C}$  signals (near 140 ppm) could be due to either or both C-13 and C-14'.] Assignment of the C-9' carbon chemical shift follows from the cross-peak (I) with 11'-H and the cross-peak (J) links 11-H with C-9 (three-bond couplings).

Since a narrow window (101–163 ppm) was used in the acquisition of the HMBC spectrum, fold-in peaks due to the methyl carbons also appeared in the olefinic carbon range (observed  $\delta$ 's near 117; actual, near 13.0). Fig. 3 shows three-bond coupling of each  $\text{CH}_3$  carbon with two chain protons; e.g. 13- $\text{CH}_3$  ( $\delta$  = 12.82) and 12-H and 14-H. Stronger cross-peaks are observed when the central carbon atoms are connected by a single bond (e.g. A,  $\delta$  = 12.82) rather than by a double bond (B,  $\delta$  = 12.98 ppm). Further, coupling of the methyl



protons with chain carbons, all of whose chemical shifts were then established, led to the assignments of these proton  $\delta$  values. Both three- and two-bond couplings ( $\text{C}=\text{C}-\text{CH}_3$ ,  $\text{C}-\text{C}-\text{CH}_3$  and  $\text{C}=\text{C}-\text{CH}_3$ ) were observed; the last gave stronger cross-peaks.

NMR spectra of **2** were similarly analysed. Proton chemical shifts are in close agreement with those previously reported.<sup>10</sup>

*Correlation of  $^{13}\text{C}$  Chemical Shift and Electron Density.*—From the data in Table 3 it can be seen that, compared to **3**, starting with C-5, every other (indicated by a dot in structure **2**) carbon is deshielded, whereas the other chain carbons are shielded. The magnitude of both effects increases the closer a given carbon is to the terminal electron-withdrawing group. Similar trends are observed for **2**, but the magnitudes are somewhat smaller.

Such shifts have been previously observed and were exploited in assigning  $^{13}\text{C}$  chemical shifts of  $\beta$ -carotene to the limiting values derived from the shifts of the corresponding carbons in apocarotenals containing 3–10 chain double bonds.<sup>13</sup> It may be noted that the reverse assignment of C-9 and C-13 for **3** was later established by COLOC.<sup>14</sup> It was suggested that the changes in chemical shifts of a particular carbon (C-5 to C-15) should correlate with changes in electron density as a function of the number of double bonds separating the aldehyde group and that carbon.<sup>13</sup> Later it was shown that the effect of the aldehyde on  $^{13}\text{C}$  chemical shifts of carbons 5–15 can be described by the  $\pi$ -electron distribution (PPP-calculation) and that contributions of other factors can be eliminated by subtracting the values for  $\beta$ -carotene, i.e.  $\Delta\delta^{13}\text{C} = 175 \Delta q_\pi$  (correlation coefficient,  $r = 0.956$ ).<sup>15</sup>

When AM1 geometry-optimized calculated electron densities are used, such a  $\Delta\delta/\Delta q$  plot (Fig. 4) shows the following.

(a) Data for **1** and **2** do not fall on the same line, and for each compound values describing the less electronegative (indicated by dots in structure **2**) carbons yield a straight line which has a much greater slope than the line joining those of the other carbons. The difference with the previous results<sup>15</sup> is attributed to two factors. First, our chemical shifts were obtained at much lower concentrations (0.03–0.06 mol  $\text{dm}^{-3}$  rather than 30–60%)

**Table 3**  $^{13}\text{C}$  Chemical shifts and excess electron densities of compounds 1–3

Atom	$\delta^{13}\text{C}$			Excess electron density (a.u.)		
	1 <sup>a</sup>	2	3 <sup>b</sup>	1 <sup>c</sup>	2	3
5	129.76	129.59	129.37	-0.0792	-0.0795	-0.0808
6	137.86	137.87	138.07	-0.0732	-0.0730	-0.0720
7	127.59	127.22	126.74	-0.1067	-0.1073	-0.1097
8	137.55	137.63 <sup>d</sup>	137.82	-0.1461	-0.1458	-0.1434
9	137.47	136.91	136.03	-0.0519	-0.0528	-0.0569
10	130.60	130.64	130.89	-0.1423	-0.1416	-0.1379
11	126.92	126.21	125.10	-0.1138	-0.1149	-0.1206
12	136.68	136.84	137.31	-0.1359	-0.1347	-0.1295
13	139.92	138.64	136.50	-0.0489	-0.0507	-0.0602
14	131.87	131.87	132.45	-0.1413	-0.1390	-0.1306
15	134.67	133.03	130.06	-0.1062	-0.1096	-0.1232
15'	129.07	129.12	130.06	-0.1382	-0.1353	-0.1232
14'	140.03	137.59 <sup>d</sup>	132.45	-0.1052	-0.1100	-0.1306
13'	135.47	135.13	136.50	-0.0833	-0.0787	-0.0602
12'	149.30	145.97	137.31	-0.0863	-0.0907	-0.1295
11'	122.44	122.63	125.10	-0.1615	-0.1569	-0.1206
10'	150.38	149.34	130.89	-0.0651	-0.0477	-0.1379
9'	131.93	136.68	136.03	-0.1388	-0.2042	-0.0569
8'	161.75	194.54	137.82	+0.0055	+0.2111	-0.1434

<sup>a</sup> Other  $\delta$  values: CN, 115.60 and 113.95; 5-CH<sub>3</sub>, 21.75; 1-CH<sub>3</sub>'s, 28.97; 9-CH<sub>3</sub>, 12.82; 13-CH<sub>3</sub>, 12.98; 13'-CH<sub>3</sub>, 12.65. <sup>b</sup> From ref. 19, except for C-9 and C-13 which were assigned by their similarity to the shifts in C<sub>6</sub>D<sub>6</sub>. <sup>c</sup> Values were previously reported with only two significant figures. <sup>d</sup> Values may be interchanged.

<sup>d</sup> Values may be interchanged.

and individual carbons are affected to different extents upon dilution. Second, the more sophisticated AM1 geometry-optimized calculations give total valence electron densities rather than  $\pi$ -electron densities derived by the PPP-method.

(b) Values derived for carbons closer than C-15 to the electron-withdrawing groups (*i.e.*, carbons 15'–10') fall on the same lines as values for carbons 5–15. (Chemical shifts of C-8' and C-9' are subject to neighbouring anisotropy effects which are different in 1 and 2 than in 3 and their  $\Delta\delta$  deviate.)

(c) For a given electron density difference, the carbons indicated by dots in structure 2 are more deshielded in 1 than the corresponding atoms in 2; the other carbons are less shielded in 1 than in 2. This result may be due to the presence of an additional C–C double bond in 1 as well as the presence of different end groups which withdraw electrons to different extents.

## Experimental

Mass spectra were obtained with a VG Autospec E spectrometer. NMR spectra (CDCl<sub>3</sub>; Me<sub>4</sub>Si) were determined with Bruker AM360 (<sup>1</sup>H, 360.13 MHz, <sup>13</sup>C, 90.56 MHz, 5 mm <sup>1</sup>H/<sup>13</sup>C dual probe) or AM500 (500.13 MHz) instruments. The COSY,<sup>16</sup> HETCOR<sup>17</sup> and HMBC<sup>18</sup> spectra were obtained according to standard procedures.

Details of the AM1 molecular orbital calculations with geometry optimization were previously reported<sup>6</sup> for compounds 1 and 2. The molecular mechanics optimized geometry was obtained using SYBYL from Tripos Associates, Inc.

Compound 2 was obtained from Roche Vitamins and Fine Chemicals. Silica gel 60 (70–230 mesh) and TLC plates (Kieselgel 60 F<sub>254</sub>, 0.2 mm) were purchased from EM Science; elution solvents were HPLC grade (Fisher). Nitrogen (Matheson, prepurified) was passed through a column of *ca.* 2 × 6" Drierite and 2 × 1" 3 Å Linde sieves. All manipulations were carried out as rapidly as possible in near-darkness, and solvents were evaporated under reduced pressure at < 35 °C.

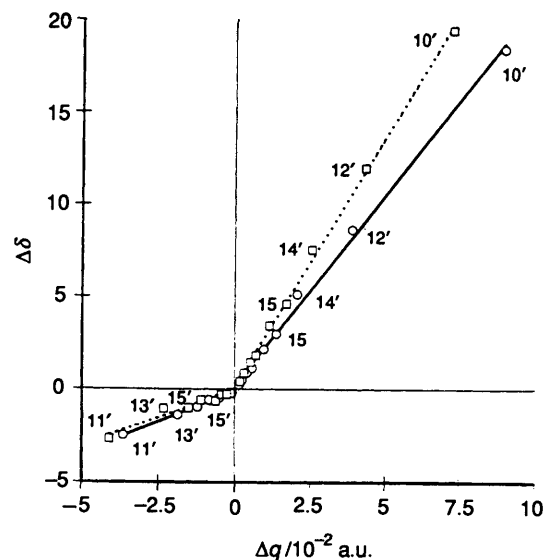


**Fig. 4** Observed difference in  $^{13}\text{C}$  NMR chemical shifts of 1 and 2 and  $\beta$ -carotene ( $\delta 1$  or  $2 - \delta 3$ ) plotted vs. the difference in calculated (AM1) electron density ( $q1$  or  $2 - q3$ ) for carbon atoms 5–10';  $\square$ : 1,  $\circ$ : 2. Slopes (and correlation coefficients) are for 1:  $0.583 \times 10^2$  (0.971) and  $2.69 \times 10^2$  (0.999); for 2:  $0.666 \times 10^2$  (0.997) and  $2.07 \times 10^2$  (0.998).

**Synthesis of 1.**—A stirred solution of 2 (0.61 g, 1.46 mmol) in dry benzene (30 cm<sup>3</sup>) in an Al-foil wrapped flask and under N<sub>2</sub> was treated with malononitrile (0.25 g, 3.8 mmol, 2.6 equiv.) followed by piperidine (0.20 cm<sup>3</sup>, 2 mmol, dried over 4 Å molecular sieves). After 3.2 h, the supernatant was decanted, residual materials were extracted with benzene (3 × 5 cm<sup>3</sup>), the combined solutions were evaporated, and the residue was at once subjected to chromatography (150 g silica gel, 7:3 CH<sub>2</sub>Cl<sub>2</sub>:CCl<sub>4</sub>). Early yellow or pale purple eluates were discarded. Later homogeneous fractions (TLC, benzene, *R<sub>f</sub>* *ca.* 0.75) were evaporated to give 1 (0.41 g) as a deep purple solid, m.p. 180 °C. Since <sup>1</sup>H NMR analysis showed the presence of H<sub>2</sub>O and TLC showed the presence of several trace impurities, a CH<sub>2</sub>Cl<sub>2</sub> solution of the solid was dried (MgSO<sub>4</sub>), filtered, and evaporated. Chromatography (75 g silica gel, topped with 10 cm<sup>3</sup> anhydrous MgSO<sub>4</sub>) under slight pressure (N<sub>2</sub>) gave pure 1 (0.39 g, 57%). For prolonged storage at -20 °C, the material was dried (1  $\mu\text{mHg}$ ; 25 °C; 0.5 h, then 35 °C; 0.5 h) in ampoules which were then cooled in liquid N<sub>2</sub> and sealed *in vacuo*. [HRMS (EI, 70 eV) Found: 464.3186. Calcd. for C<sub>33</sub>H<sub>40</sub>N<sub>2</sub>: 464.3192.]

## Acknowledgements

This work was supported by the Division of Chemical Sciences, Office of Basic Energy Sciences, Department of Energy under Grant No. DE-FG05-86ER13465. Kim Ouderkerk is thanked for assistance in purifying 2 and Mazen Khaled for calculations of the electron densities for 1. The Alabama supercomputer network is acknowledged for a very generous allocation of Cray XMP-24 computer time and Tripos Associates, Inc. for a grant for SYBYL molecular modelling software. Roche Vitamins and Fine Chemicals, Nutley, NJ, is thanked for providing a sample of a 20% oil suspension of compound 2.

## References

- 1 D. Siefertmann-Harms, *Biochim. Biophys. Acta*, 1985, **811**, 325; K. Sauer, *Bioenergetics of Photosynthesis*, Academic Press, New York, 1975, pp. 115–181.
- 2 *Carotenoid Chemistry and Biochemistry*, eds. G. Britton and T. W. Goodwin, Pergamon Press, New York, 1981.

- 3 E. Fuginiori and M. Tavla, *Photochem. Photobiol.*, 1966, **5**, 877; C. S. Foote and R. W. Denny, *J. Am. Chem. Soc.*, 1968, **90**, 6233.
- 4 P. Mathis and C. Schenck, in *Carotenoid Chemistry and Biochemistry*, eds. G. Britton and T. W. Goodwin, Pergamon Press, New York, 1981, p. 339.
- 5 B. W. Chadwick and H. A. Frank, *Biochim. Biophys. Acta*, 1986, **851**, 257.
- 6 M. P. O'Neil, M. R. Wasielewski, M. M. Khaled and L. D. Kispert, *J. Chem. Phys.*, 1991, **95**, 7212.
- 7 M. R. Wasielewski, D. G. Johnson, E. G. Bradford and L. D. Kispert, *J. Chem. Phys.*, 1989, **91**, 6691.
- 8 W. Svec and M. R. Wasielewski, personal communication.
- 9 H. Ikeda, T. Sakai and Y. Kawabe, Jpn P 02 002 534; *Chem. Abstr.*, 1990, **113**, 49536v.
- 10 G. Vetter, G. Englert, N. Rigassi and U. Schwieter in *Carotenoids*, ed. O. Isler, Birkhäuser Verlag, Basel, Switzerland, 1971, Chapter IV.
- 11 J. Wernly and J. Lauterwein, *J. Chem. Soc., Chem. Commun.*, 1985, 1221.
- 12 E. Breitmaier and W. Voelter, *Carbon-13 NMR Spectroscopy*, 3rd edn. VCH Verlagsgesellschaft, Weinheim, Germany, 1987, p. 336.
- 13 W. Bremser and J. Paust, *Org. Magn. Reson.*, 1974, **6**, 433.
- 14 J. Wernly and J. Lauterwein, *J. Magn. Reson.*, 1986, **66**, 355.
- 15 R. Wolff and R. Radeglia, *Z. Phys. Chem.*, 1982, **263**, 199.
- 16 M. Rance, O. W. Sørensen, G. Bodenhausen, G. Wagner, R. R. Ernst and K. Wüthrich, *Biochem. Biophys. Res. Commun.*, 1983, **117**, 479.
- 17 A. Bax, *J. Magn. Reson.*, 1983, **53**, 517.
- 18 A. Bax and M. F. Summers, *J. Am. Chem. Soc.*, 1986, **108**, 2093.
- 19 J. Wernly and J. Lauterwein, *Magn. Reson. Chem.*, 1985, **23**, 170.

Paper 2/06356E

Received 27th November 1992

Accepted 15th December 1992